

A COMPARATIVE STUDY OF FAILURE CRITERIA IN SHEET METAL FORMING ANALYSIS

NGOC-TRUNG NGUYEN, DAE-YOUNG KIM AND HEON YOUNG KIM

Department of Mechanical and Biomedical Engineering, Kangwon National University,
192-1, Hyoja2-dong, Chuncheon, Gangwon-do, 200-701, Korea
e-mail: ntnguyen@kangwon.ac.kr, dae-young@kangwon.ac.kr, khy@kangwon.ac.kr
Web page: cae.kangwon.ac.kr

Key words: Sheet Metal Forming, Formability, Failure Criteria, Necking, Ductile Fracture.

Abstract. Development of predictive capabilities of forming failure can help not only to reduce the experimental effort of formability characterization but also to accelerate the development of new or improved sheet metal alloys. This paper presents a comparative study on prediction of failures in sheet metals which leads to undesirable localized straining and/or fracture during the stamping process. The theoretical diffuse and localized necking models were applied. Several classical fracture criteria were also studied in the finite element analysis. All these models were used to predict the onset of failure and compare with the experimental cases. Comparison and validity of different failure criteria was discussed.

1 INTRODUCTION

In sheet metal forming analysis, the criterion using Forming Limit Diagram (FLD) is widely used for failure prediction since it was originally introduced by Keeler (1965) and Goodwin (1968) [1, 2]. FLD has been commonly applied to evaluate the formability of sheet metals for diagnosing the possible production problems in sheet metal stamping. It indicates the limit strains corresponding to the onset of localized necking over a range of major-to-minor strain ratios. Although the concept of FLD is simple, its experimental implementation is not trivial. Therefore, analytical and numerical predictions of FLD have been intensively studied as the alternative methods. Recently, ductile fracture criteria have been used to determine the limit forming states [3]. The limit states were calculated by plugging the values of stress and strain histories obtained from the simultaneous finite element simulations into the integral form of different ductile fracture criteria. Several successful predictions for the fracture process have been reported. Some fracture criteria can be used to determine the FLD successfully whereas some others fail with this effort.

This paper presents a comparative study on prediction of failures in sheet metals which leads to undesirable localized straining and/or fracture during the stamping process. More detailed discussion on each single topic can be found in [4, 5]. The theoretical diffuse and localized necking models according to Swift-Hill (1952) and Stören-Rice (1975) were applied. Several classical fracture criteria such as Rice-Tracey (1969), Cockcroft-Latham (1968), Brozzo et al. (1972), Oh *et al.* (1979), and Wilkins *et al.* (1980) were also studied in the finite element analysis. All these models were used to predict the onset of failure and

compare with the experimental cases. To determine the FLD experimentally, we conducted the Nakajima tests following the ISO 12004-2 standard [6].

2 EXPERIMENT SETUP

In order to determine the FLD of metal sheet, limiting dome height (LDH) tests were performed. The die set of the NUMISHEET '96 benchmark model was used. Experimental setup including the formability tester and the die set is depicted in Fig. 1. Four kinds of specimens were cut into so-called Nakajima specimens from the same material sheet, the narrowest widths of which were 25, 50, 75 and 175mm, with a length of 175mm in the rolling direction. Fig. 2 shows different blank shapes used in this study. The ASIAS scanning system was used to measure principal strains.



Figure 1: The formability tester and die set

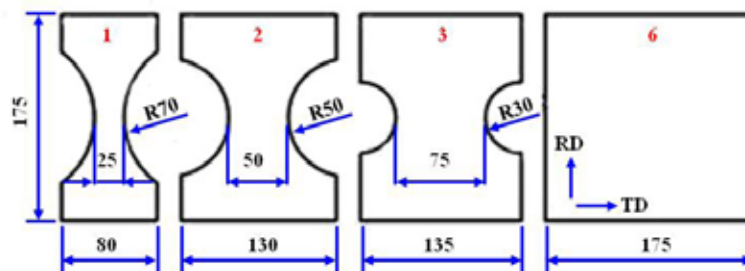


Figure 2: Blank shapes of the LDH test

3 FAILURE CRITERIA

3.1 Necking criteria

Under significant plastic deformation the onset of localization, which is often referred to as *diffuse necking*, occurs. Diffuse necking, which ends the initially uniform deformation in a wide thin sheet, involves contraction in both the lateral and width directions. The diffuse neck is accompanied by contraction strains in both the width and thickness direction and develops

gradually thus still allowing considerable extension [7]. Diffuse necking is usually predicted by, e.g. the Considère (1885) and Swift-Hill (1952) criteria [8]. Upon further deformation the necking region further localizes in an infinitesimal band which is related to the material instability or the *localized necking*. During localized necking the specimen thins without further width contraction [7]. Localized necking can be predicted by, e.g. the model of Hill (1952). Different approaches to predict necking have been introduced from different perspective views of the phenomenon, e.g. maximum load, zero extension line, bifurcation from point vertex on the yield surface or pre-existing imperfections.

Critical thinning or thickness reduction is commonly used in press shop to determine the necking and it is assumed that necking occurs when the thickness strain is around 18–20% [9]. Even though that critical thinning criterion is frequently used in industry, there is not much research has done into this area.

3.2 Fracture criteria

Based on general observations from ductile tests that the load carrying capacity is reduced during the process, the materials are considered to be damaged. Damage indicators and damage rules for the ductile materials have been defined in different ways. It is postulated that fracture occurs when the damage, D , exceed a critical value. In the normalized form, the condition of fracture is expressed as:

$$D = 1 \quad (1)$$

Cockcroft and Latham (1968) developed a ductile fracture criterion based on the concept of “true ductility” [10]. Cockcroft-Latham stated that fracture will not occur until the product of maximum principal stress and equivalent strain is accumulated to a critical value. The *reduced form* of the Cockcroft-Latham criterion is given by:

$$D = \frac{1}{D_{\text{crit.}}^{\text{C-L}}} \int_0^{\bar{\varepsilon}^f} \sigma_1 d\bar{\varepsilon}^p \quad (2)$$

where σ_1 is the highest tensile stress, $\bar{\varepsilon}^p$ is the equivalent plastic strain, $\bar{\varepsilon}^f$ is the equivalent fracture strain. The critical value, $D_{\text{crit.}}^{\text{C-L}}$, is determined experimentally. Brozzo *et al.* (1972) modified the Cockcroft-Latham criterion fracture condition to express the effect of principal stress and hydrostatic stress [11].

$$D = \frac{1}{D_{\text{crit.}}^{\text{B}}} \int_0^{\bar{\varepsilon}^f} \frac{2\sigma_1}{3(\sigma_1 - \sigma_m)} d\bar{\varepsilon}^p \quad (3)$$

where $\sigma_m = (\sigma_1 + \sigma_2 + \sigma_3)/3$ is the hydrostatic stress. The Cockcroft-Latham criterion was later modified by Oh *et al.* (1979) to have the so-called *normalized form* as given below [12]:

$$D = \frac{1}{D_{\text{crit.}}^{\text{Oh}}} \int_0^{\bar{\varepsilon}^f} \frac{\sigma_1}{\bar{\sigma}} d\bar{\varepsilon}^p \quad (4)$$

Wilkins *et al.* (1980) suggested a damage function that includes a hydrostatic pressure weighting term, w_1 , and an asymmetric-strain weighting term, w_2 . Fracture is postulated to occur when the damage function D exceeds a critical value D_C over a critical material volume R_C , leading to discontinuous macro crack creation and stepwise growth [13]. The criterion is rewritten in the normalized form as:

$$D = \frac{1}{D_{\text{crit.}}^{\text{W}}} \int_0^{\bar{\varepsilon}^f} w_1 w_2 d\bar{\varepsilon}^p \quad (5)$$

The hydrostatic pressure weighting term accounts for the growth of holes during loadings that consists of large stress triaxiality and small strain. The asymmetric-strain weighting term accounts for the observation that, after initiation, the holes can link up as a band if subsequent loading is shear. The two weighting terms are defined by:

$$w_1 = \left(\frac{1}{1 - a\sigma_m} \right)^\alpha; \quad w_2 = (2 - A)^\beta \quad (6)$$

where a is a constant and relates to a so-called limit pressure, P_{lim} ; A is the asymmetric-strain factor. These terms are calculated by:

$$a = \frac{1}{P_{\text{lim}}}; \quad A = \max \left(\frac{s_2}{s_3}, \frac{s_2}{s_1} \right), \quad s_1 \geq s_2 \geq s_3 \text{ are deviatoric stresses} \quad (7)$$

4 RESULTS AND DISCUSSION

The aluminum alloy (AA6061-T6) sheet of 0.8mm thickness was used to prepare specimens for the experimental tests in this paper. The mechanical properties and material constants are obtained from the tensile test of flat type dog-bone and shear specimens as shown in Fig. 3. The inverse method was applied to determine the failure strains at fracture of the tensile specimen using finite element simulation. The analysis was conducted with the assumptions that the material is isotropic and follows the von Mises plasticity theory.

The fracture uniaxial tensile test of the dog-bone specimens could not only provide the information about stress-strain relation and the fracture strains of the material but also help to calculate the material parameters through the inverse method with stress and strain result outputs of a parallel finite element simulation. As an example, the thickness strain record of the loaded specimen was used to identify the critical thinning value which was later applied as a criterion to predict failure. Such process is illustrated in Fig. 4 which shows the bifurcation point as failure occurs.

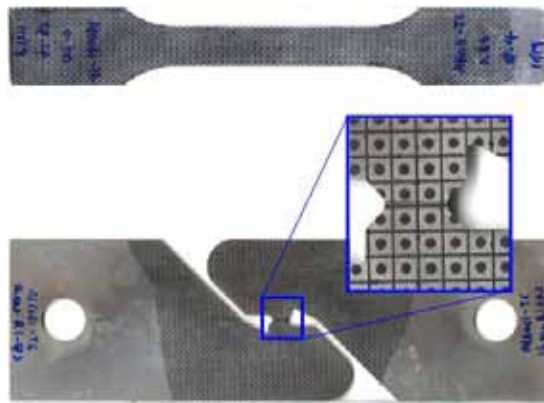


Figure 3: Dog-bone and shear specimens

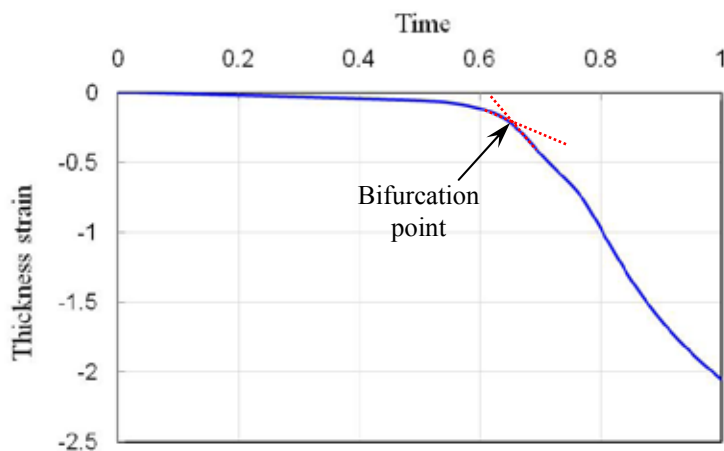


Figure 4: Determination of the failure point using the thickness strain record

The experiment data and the FLD of AA6061-T6 obtained from the reference paper [14] are given in Fig. 5. The experimental data and the reference FLD agree pretty well except for the proximity of biaxial stretch mode. The calculated limit strains using necking criteria together with the experimental FLD from reference [14] are shown in Fig. 6. The left-hand side of the experimental FLD is parallel to the calculated curve for localized necking by Hill's criterion. For positive values of ε_2 , the calculated curve using Swift's criterion has similar shape and is in accord with the experimental one. In both sides, the experimental curve is higher than the analytical ones. The Stören-Rice curve approaches the experimental FLD in the modes of uniaxial tension and biaxial stretch. But for plane strain condition, it predicted the limit strain that is far below the true value. It reflects a fact that necking has developed much earlier than it can be detected as depicted in Fig. 6 (a). An identical observation was reported for the forming limit diagram of a low-carbon steel [7].

Applying the inverse method for the finite element simulation of the tensile test of this material, the flat type dog-bone specimen failed at about 21.5% thickness strain. Limit strains of the 17.5, 20, 22.5 and 25% thickness strains conditions were also obtained from the finite element simulation and shown in Fig. 6 (b). On the left side of FLD, necking occurs when the thickness strain is about 20%. It is reasonable to predict localized necking occurs before the

critical value of thickness strain at which the material was failed in the tensile test. However, the thinning criterion underestimated failures on the right hand side of FLD.

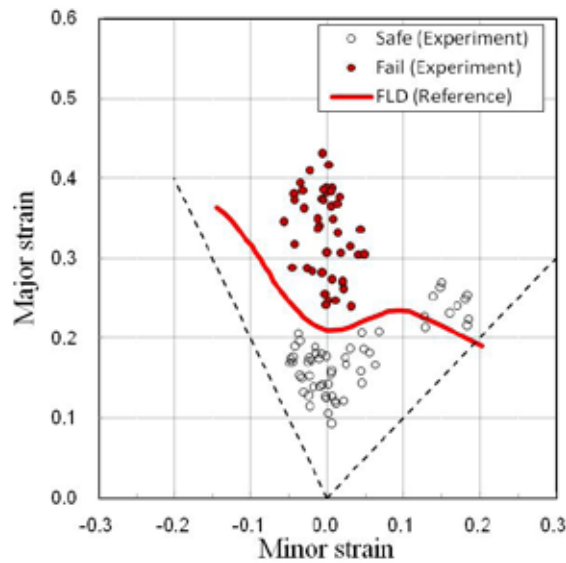


Figure 5: The forming limit diagram: experimental results and the reference FLD

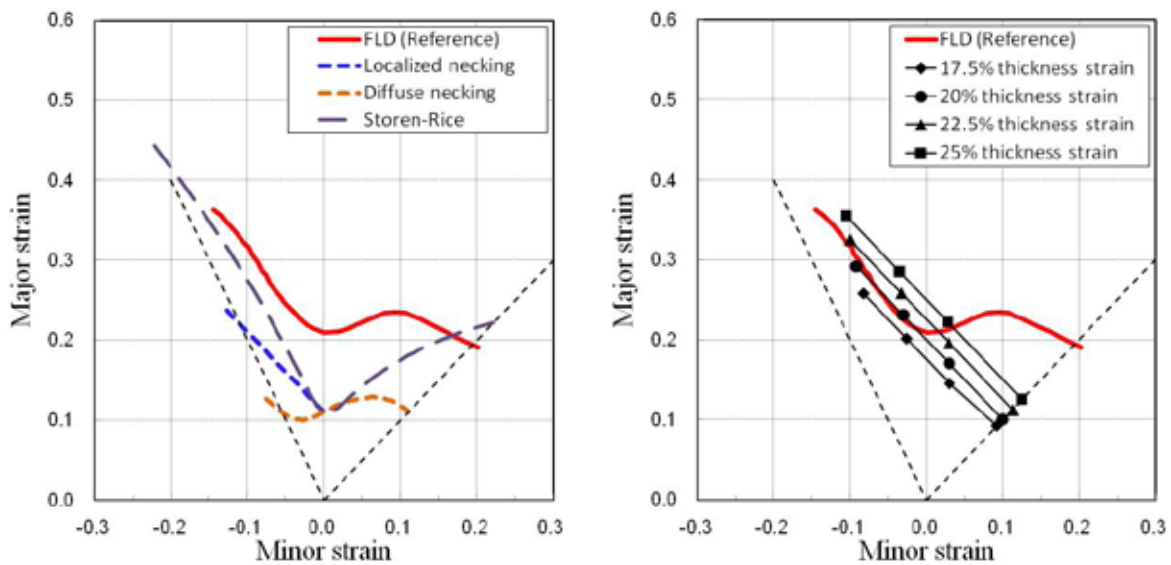


Figure 6: Predictions of the FLD: (a) with necking criteria, (b) with thinning criterion

Comparison between limit strain due to ductile fracture criteria and that of the experimental FLD is given in Fig. 7. Only predictions with the criteria proposed by Rice-Tracey, Brozzo *et al.*, Oh *et al.*, and Wilkins *et al.* are presented. More criteria including the proposed criterion by the present authors are discussed in [5]. The calculated strains of all models are located on or above the FLD. This makes sense as necking, which is followed by fracture, occurs earlier than the observed fracture. Among the four investigated fracture models in this study, the Wilkins *et al.* criterion is able to predict pretty well the forming

limit. Other models seem to overestimate the failure strains. Besides, as can be seen from Fig. 7, the distance from the fracture points to the FLD following Wilkins *et al.* is relative small reflecting the experimental observation that soon after necking fracture occurs. Especially, for uniaxial and biaxial stretch modes fracture follows almost right after necking.

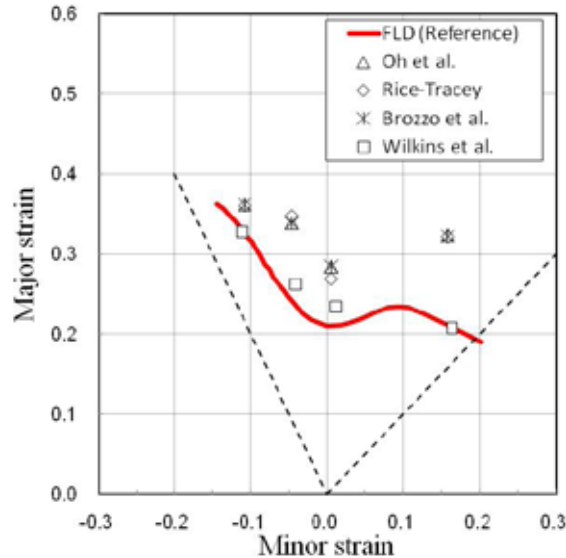


Figure 7: Predictions of the FLD using ductile fracture criteria

5 SUMMARY

Failures in the LDH tests were predicted by several necking and ductile fracture criteria in order to establish a calculated FLD and then compare that with the experimental curve. The following conclusions were made:

- Swift and Hill necking criteria underestimated the limit strains but these calculated curves have the similar shape with the FLD.
- The left side of the FLD was well predicted by thinning and the Wilkins *et al.* criterion.
- Whereas the neighbor of uniaxial and biaxial stretch modes can be calculated by Stören-Rice criterion, the prediction for plane strain condition is far to be satisfied.
- In all cases, the ductile fracture criteria tended to overestimate the failure which is initiated by necking in practice. Even though the calculated FLD is not well shaped, the prediction by the Wilkins *et al.* fracture criterion for the low ductility material in this study is acceptable.
- At the current time the work on sensitivity of the forming limit with different yield conditions is undertaken.

ACKNOWLEDGEMENTS

This work was supported by the Basic Science Research Program (2010-0017090) and the World Premiere Materials program (10037929) funded by the Korean government (Ministry of Education, Science and Technology, and Ministry of Knowledge Economy).

REFERENCES

- [1] Keeler, S. P., and Backhofen, W. A., Plastic instability and fracture in sheet stretched over rigid punches. *ASM Transactions Quarterly* (1964) **56**: 25-48.
- [2] Goodwin, G. M. Application of strain analysis to sheet metal forming in the press shop. *SAE technical paper 680093* (1968).
- [3] Ozturk, F., and Lee, D. A New Methodology for Ductile Fracture Criteria to Predict the Forming Limits. *Journal of Materials Engineering and Performance* (2007) **16**(2): 224-228.
- [4] Nguyen, N.-T., Kim, D.-Y., and Kim, H. Y. Numerical prediction of failure in sheet metal forming process: Part I. Necking (in preparation). (2011).
- [5] Nguyen, N.-T., Kim, D.-Y., and Kim, H. Y. Numerical prediction of failure in sheet metal forming process: Part II. Ductile fracture (in preparation). (2011).
- [6] International Standard, ISO 12004-2:2008 (E).
- [7] Hosford, W. F., and Caddell, R. M. *Metal Forming: Mechanics and Metallurgy*. Cambridge University Press, New York, (2007).
- [8] Considère, M. L'emploi du fer et de l'acier dans les constructions. *Ann. Ponts Chausseés* (1885) **9**: 574-775.
- [9] Esche, S. K., Kinzel, G. L., and Altan, T. *Review of failure analysis in sheet metal forming simulation*. In: J. K. Lee, G. L. Kinzel, and R. H. Wagoner (Eds.), *Proceedings of the Numisheet '96*. Dearborn, Michigan, USA (1996): 270-279.
- [10] Cockcroft, M. G., and Latham, D. J. Ductility and the workability of metals. *Journal of the Institute of Metals* (1968) **96**: 33-39.
- [11] Brozzo, P., de Luca, B., and Rendina, R. *A new method for the prediction of formability in metal sheets*. In: (Eds.), *Proceedings of the Proceedings of the Seventh Biennial Conference of International Deep Drawing Research Group on Sheet Metal Forming and Formability*. (1972).
- [12] Oh, S. I., Chen, C. C., and Kobayashi, S. Ductile Fracture in Axisymmetric Extrusion and Drawing. *J. Eng. Ind. Trans. ASME* (1979) **101**: 36-44.
- [13] Wilkins, M. L., Streit, R. D., and Reaugh, J. E. Cumulative-strain-damage model of ductile fracture: simulation and prediction of engineering fracture tests. Lawrence Livermore National Laboratory, Report UCRL-53058, (1980).
- [14] Djavanroodi, F., and Derogar, A. Experimental and numerical evaluation of forming limit diagram for Ti6Al4V titanium and Al6061-T6 aluminum alloys sheets. *Materials & Design* (2010) **31**(10): 4866-4875.